Volume 17
Number 6
11 February 2026
Pages 2883–3362

Chemical Science

rsc.li/chemical-science

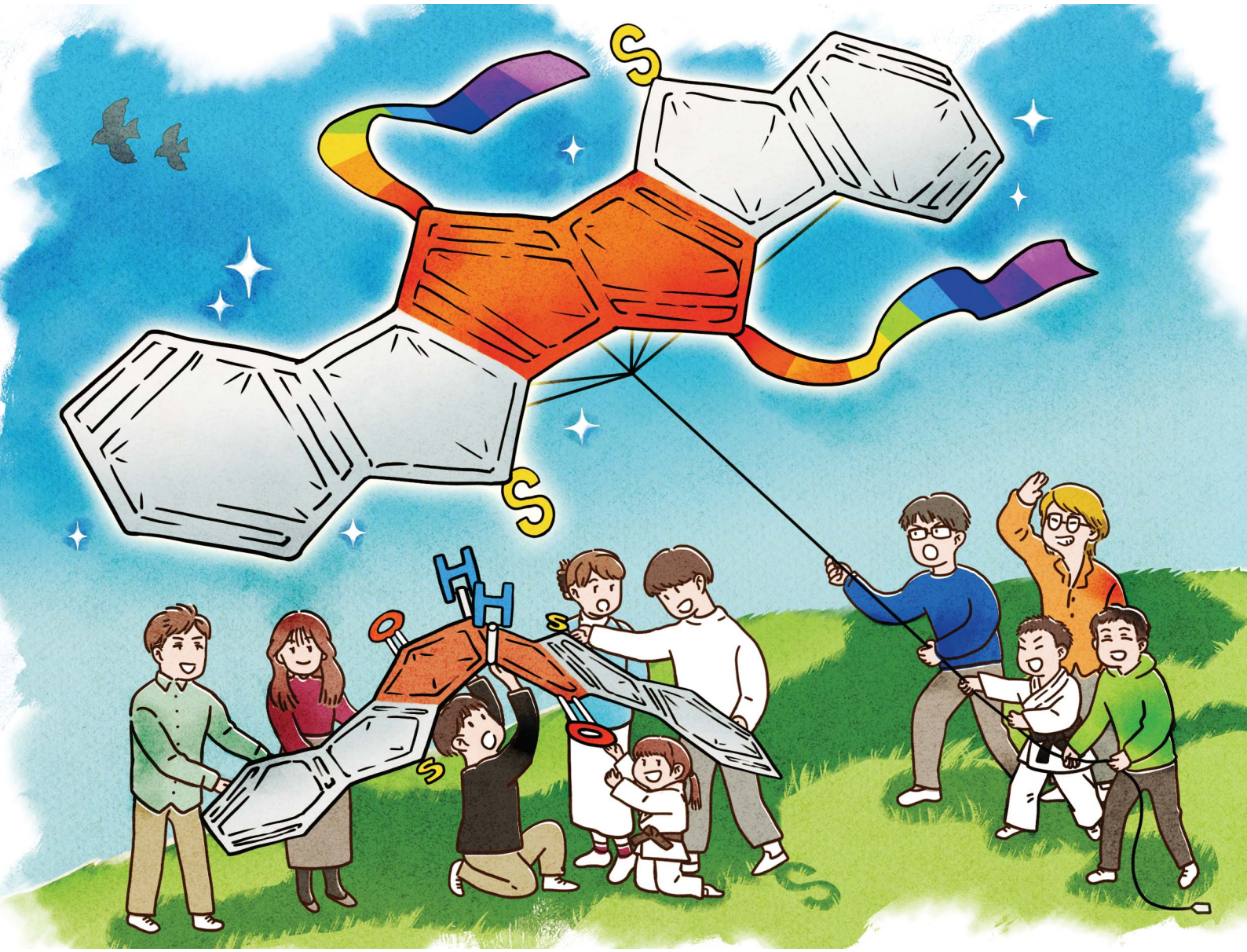

ISSN 2041-6539

ROYAL SOCIETY OF CHEMISTRY

EDGE ARTICLE

Aiko Fukazawa *et al.*

Modular synthesis of benzothiophene-fused pentalenes reveals substituent-dependent antiaromaticity

Chemical Science

ROYAL SOCIETY OF CHEMISTRY

EDGE ARTICLE

View Article Online
View Journal | View Issue

Cite this: *Chem. Sci.*, 2026, **17**, 3005

All publication charges for this article have been paid for by the Royal Society of Chemistry

Modular synthesis of benzothiophene-fused pentalenes reveals substituent-dependent antiaromaticity

Ryosuke Isogai, [a] Kosuke Yasui †[b] and Aiko Fukazawa *[b]

Received 28th November 2025
Accepted 9th January 2026

DOI: 10.1039/d5sc09325b

rsc.li/chemical-science

Antiaromatic π-electron systems provide unique electronic features arising from the cyclic conjugation of 4n π-electrons, yet synthetic access to strongly antiaromatic heteroarene-fused scaffolds remains limited. Here we report a general synthetic route to benzothiophene-fused pentalenes *via* the first thiophene analogue of Brand's bicyclo[3.3.0]octadiene-2,6-dione intermediate. The pre-installation of the bicyclic five-membered-ring core at an early stage of synthesis enables efficient annulation of benzothiophene moieties and late-stage diversification at the 1,4-positions through the 1,2-addition of organometallic nucleophiles, followed by optimized dehydration. This strategy affords a series of benzothiophene-fused pentalenes bearing diverse aryl, heteroaryl, and alkynyl substituents in practical yields, with isolation by simple filtration. The benzothiophene-fused pentalenes thus obtained exhibit strong antiaromatic character that correlates with electronic effects, consistent with the topological charge stabilization rule. This work establishes a versatile platform for probing substituent-dependent antiaromaticity and for designing functional materials based on strongly antiaromatic π-systems.

Introduction

Antiaromatic π-electron systems exhibit distinct electronic properties such as narrow HOMO–LUMO gaps,[1] amphoteric redox behavior,[2] and low-lying triplet excited states,[3,4] making them attractive frameworks for optoelectronic materials.[5] Among these, pentalene (**1**), a bicyclic conjugated hydrocarbon with two fused five-membered rings, is a prototypical antiaromatic framework (Fig. 1a, top).[6] Owing to its planarity and minimal bond-angle strain among 4n π-electron hydrocarbons, pentalene and its derivatives have been considered promising building blocks for functional materials.[7] To exploit the characteristic properties of pentalene derived from its antiaromatic character, a variety of annulated derivatives have been developed.[8–33] Dibenzo[*a*,*e*]pentalene (**2**) and its derivatives have been most extensively investigated due to their high stability,[8–23] although the strong aromatic character of benzene rings diminishes the antiaromatic character of the pentalene cores (Fig. 1a, bottom left). In contrast, the annulation with weakly aromatic heteroarenes such as thiophene preserves the antiaromatic character of pentalene,[24,25] giving rise to dithieno[*a*,*e*]pentalene (**3**),[11a,12b,25,26] benzothiophene-fused (**4**), and its π-expanded analogues[22e] as thermally stable compounds (Fig. 1a, bottom right). These heteroarene-fused pentalenes offer an attractive platform for optoelectronic materials, yet their synthesis remains challenging due to the lack of general and efficient synthetic methods.

Previous synthetic routes for dibenzo[*a*,*e*]pentalenes were mostly based on intra- or intermolecular cyclization of phenylacetylenes (Fig. 1b).[9–18] However, analogous reactions with thiophene-based substrates have generally failed or afforded poor yields (Fig. 1b).[25,31] We hypothesized that these difficulties stem primarily from increased ring strain and higher reactivity of strongly antiaromatic dithieno[*a*,*e*]pentalene under the reaction conditions. Indeed, our recent studies indicated that benzothiophene-fused pentalenes can strongly coordinate to Ni(0),[34] inhibiting the desired reaction.

To overcome these limitations, we revisited the classical strategy, which constructs the pentalene framework from a benzannulated bicyclo[3.3.0]octadiene-2,6-dione precursor (**5**, Fig. 1b). This method, originally reported by Brand in 1912,[8] and recently refined by Esser and co-workers,[20,21] enables transition metal-free formation of the dibenzo[*a*,*e*]pentalene framework. We herein report the development of a new synthetic route of benzothiophene-fused pentalenes **4** *via* the corresponding benzothiophene-fused bicyclo[3.3.0]octadiene-2,6-dione intermediate (**6**) derived from bicyclo[3.3.0]octane-2,6-dione **7** (Fig. 1c). This approach allows late-stage introduction of diverse substituents to the 1,4-positions of the pentalene core, affording a new family of stable yet strongly antiaromatic

[a]*Department of Energy and Hydrocarbon Chemistry, Graduate School of Engineering, Kyoto University, Yoshida, Sakyo-ku, Kyoto 606-8501, Japan*

[b]*Institute for Integrated Cell-Material Science (WPI-iCeMS), Institute for Advanced Study, Kyoto University, Yoshida, Sakyo-ku, Kyoto 606-8501, Japan. E-mail: afukazawa@icems.kyoto-u.ac.jp*

† Present address: Department of Applied Chemistry, Graduate School of Engineering, The University of Osaka, Suita, Osaka 565-0871, Japan.

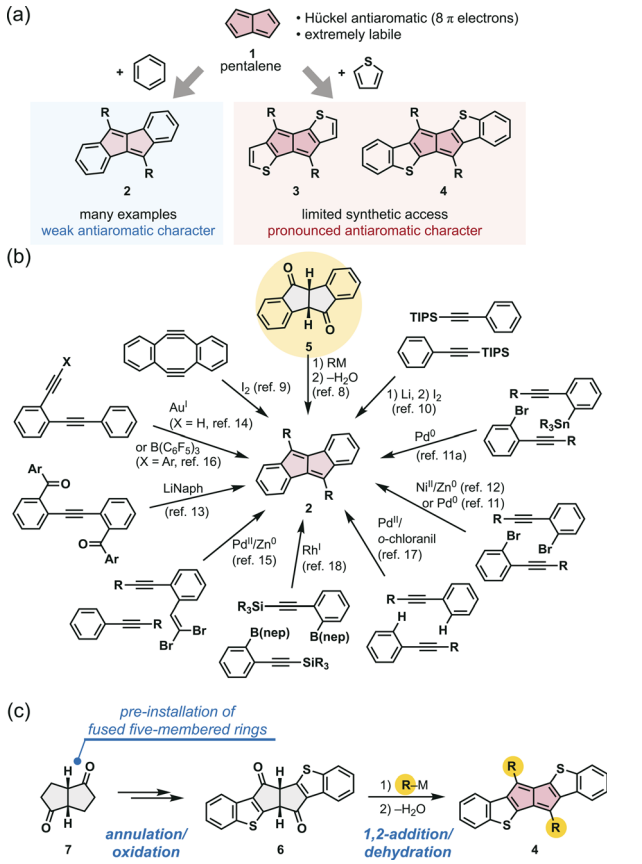

Fig. 1 (a) Effect of fused aromatic rings on the antiaromaticity of pentalene **1**. (b) Previous synthetic methodologies of dibenzo[*a*,*e*]pentalenes **2**. (c) Synthetic strategy in the present study.

compounds. The resulting compounds provide a versatile platform for elucidating the substituent effects on antiaromaticity and the corresponding physical properties.

Results and discussion

In Esser's improved synthesis of dibenzo[*a*,*e*]pentalene derivatives based on Brand's approach, the key intermediate, a benzannulated bicyclo[3.3.0]octadiene-2,6-dione **5**, was prepared in only three steps *via* dimerization of ethyl phenylacetate followed by hydrolysis and intramolecular cyclization (Fig. 2a, top).[20a,22h] However, our attempts to apply these conditions to ethyl thienylacetate failed, yielding a complex mixture rather than the desired dimer (Fig. 2a, bottom), indicating the need for an alternative synthetic strategy to access thiophene-fused analogues.

We therefore focused on the synthesis of benzothiophene-fused pentalene **4** through a new benzothiophene analogue of Brand's intermediate (**6**; Fig. 2b). Bicyclo[3.3.0]octane-2,6-dione (**7**) was chosen as the key starting material, as it embeds the fused five-membered-ring motif of the pentalene core from the outset.[35] Introducing the principal source of ring strain at an early stage of synthesis avoids the strain accumulation that hampers conventional approaches in which the pentalene core is constructed only at the end. The benzothiophene rings were

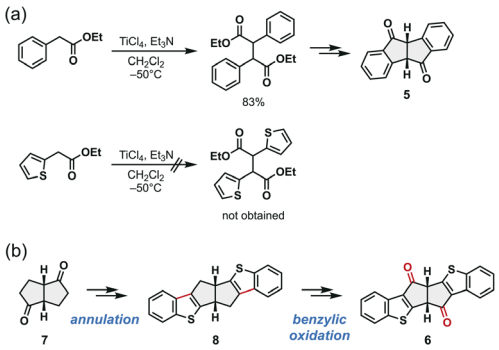

Fig. 2 (a) A previous synthetic method of benzannulated bicyclo[3.3.0]octadiene-2,6-dione **5** (top) and the result of our preliminary investigation using ethyl thienylacetate (bottom). (b) The synthetic strategy of benzothiophene-fused bicyclo[3.3.0]octadiene-2,6-dione **6** in this work.

to be constructed laterally around this scaffold to furnish the hexacyclic compound **8**, followed by benzylic oxidation to the desired diketone **6**.

Following this strategy, a benzothiophene analogue of Brand's intermediate, **6**, could be successfully synthesized as shown in Scheme 1. The Ti-mediated nucleophilic addition of 2-bromobenzothiol to **7** and subsequent dehydration[36] afforded the alkenyl sulfide **9** in 37% yield. A Pd-catalyzed intramolecular cyclization efficiently produced the benzothiophene-fused bicyclo[3.3.0]octadiene **8** in 85% yield.§ Regioselective benzylic oxidation of **8** proved challenging, yet $PhI(OAc)_2$/TBAI[37] enabled regioselective conversion to the acetoxylated intermediate **10**, which upon hydrolysis gave the desired diol **11** in 59% overall yield for two steps. Finally, PCC oxidation of **11** gave the desired diketone **6** in 73% yield. This compound represents the first thiophene-annulated analogue of Brand's intermediate and a versatile precursor to pentalene frameworks.

We next examined the construction of benzothiophene-fused pentalenes from **6**. The 1,2-addition of Grignard reagents to **6** proceeded smoothly in the presence of $CeCl_3$ under conditions essentially the same as those reported for the synthesis of dibenzo[*a*,*e*]pentalene derivatives.[20a] However, subsequent dehydration gave a different outcome, indicating that modification of the reaction conditions was required (Scheme 2). Specifically, for the preparation of benzothiophene-fused pentalene **4a** bearing 3,5-bis(trifluoromethyl)phenyl

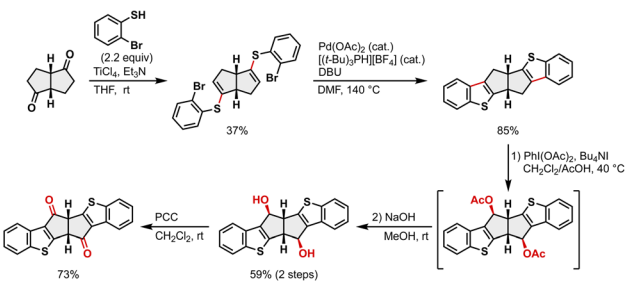

Scheme 1 Synthesis of a key intermediate **6**.

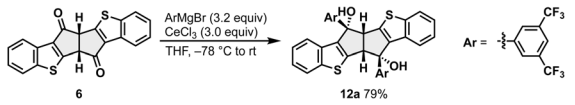

Scheme 2 Transformation of a key intermediate **6** to aryl-substituted diol **12a**.

Table 1 Effect of the equivalents of TsOH for the dehydration of **12a**

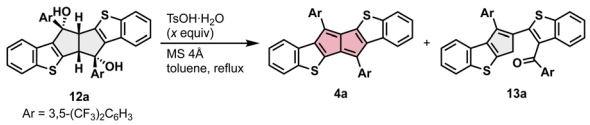

		Yield[a]	
Entry	*x*	**4a**	**13a**
1	0.1	17%	45%
2	2.0	65%	21%
3	3.0	74%	23%

[a] Isolated yield.

groups as a model compound, the corresponding Grignard reagent was subjected to the reaction with **6** in the presence of $CeCl_3$ to afford the bis(benzyl alcohol) **12a** in 79% yield (Scheme 2). In contrast, the following dehydration using the catalytic amount of $TsOH \cdot H_2O$ produced the desired pentalene **4a** in only 17% yield, with a ring-opened compound **13a** as the major product in 45% yield (entry 1 in Table 1).¶ A similar ring-opening reaction has been reported in the synthesis of a highly strained cyclophane-type dibenzo[*a*,*e*]pentalene.[21a] In line with this observation, the low yield of **4a** accompanied by the ring opening suggests that thiophene fusion introduces additional strain. Increasing the amount of $TsOH \cdot H_2O$ reversed the product ratio (entries 2 and 3), and 3.0 equivalents afforded the desired pentalene **4a** in 74% yield (entry 3).

With the optimized conditions, diverse benzothiophene-fused pentalenes **4** were synthesized from the common intermediate **6** by 1,2-addition of the corresponding Grignard reagents or organolithium reagents in the presence of $CeCl_3$ (Fig. 3). The scope includes derivatives bearing electron-withdrawing 3,5-$(CF_3)_2C_6H_3$ (**4a**), relatively neutral (Ph, **4b**), and electron-donating (4-$MeOC_6H_4$, **4c**) aryl groups, as well as heteroaryl (2-thienyl, **4d**), and triisopropylsilyl (TIPS)ethynyl groups (**4e**). Notably, the final dehydration step induced precipitation of desired products **4**, enabling facile isolation by simple filtration without chromatography. This route thus provides practical access to structurally diverse benzothiophene-fused pentalenes.

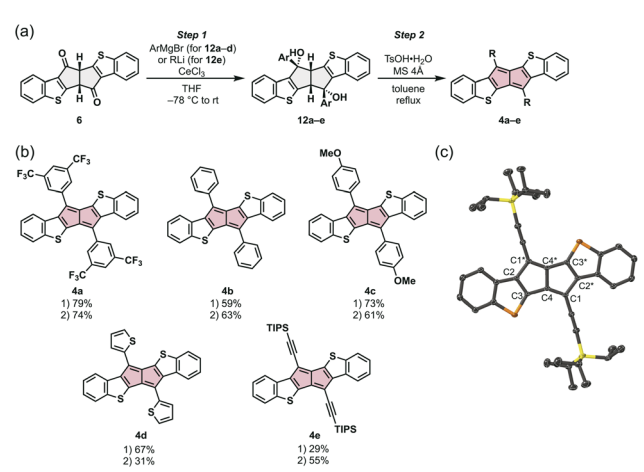

Fig. 3 Synthesis of benzothiophene-fused pentalenes **4a–e** bearing various substituents at 1,4-positions. (a) Synthetic conditions. (b) Molecular structures of **4a–e** and the isolated yields for Steps 1 and 2. TIPS = triisopropylsilyl. (c) X-ray crystal structure of **4e** (thermal ellipsoids drawn at 50% probability; black: carbon, orange: sulfur, yellow: silicon). Hydrogen atoms and the minor disordered components are omitted for clarity. Selected bond lengths: C1*–C2 = 1.490(2) Å, C2–C3 = 1.382(2) Å, C3–C4 = 1.452(2) Å, C4–C1 = 1.375(2) Å.

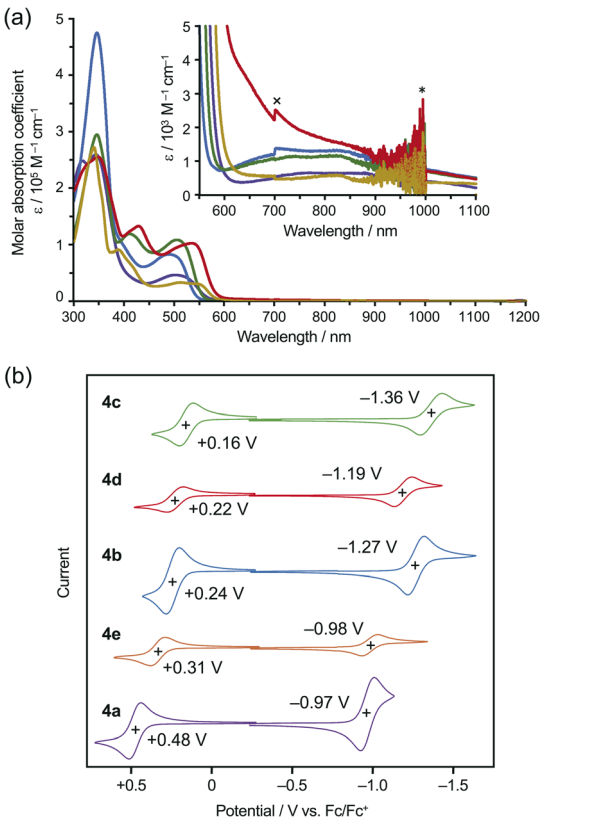

Fig. 4 Photophysical and electrochemical properties of benzothiophene-fused pentalenes **4a–e**. (a) UV/Vis/NIR electronic absorption spectra of **4a** (purple), **4b** (blue), **4c** (green), **4d** (red), and **4e** (beige) in THF. In the inset spectra, minor discontinuities around 700 nm (marked with ×) arise from the grating changeover of the spectrophotometer, and the increased noise near 900 nm (marked with *) is due to the detector sensitivity around the PMT–InGaAs switching wavelength (~830 nm). (b) Cyclic voltammograms of **4a–e** in THF and CH_2Cl_2 (0.5 mM) for reductive and oxidative regions, respectively; scan rate: 50 mV s^{-1}, supporting electrolyte: [*n*-Bu_4N][PF_6] (0.1 M). All potentials referenced *vs.* Fc/Fc^+. The plus (+) signs indicate the half-wave potentials ($E_{1/2}$) of the reversible redox waves in the cyclic voltammograms.

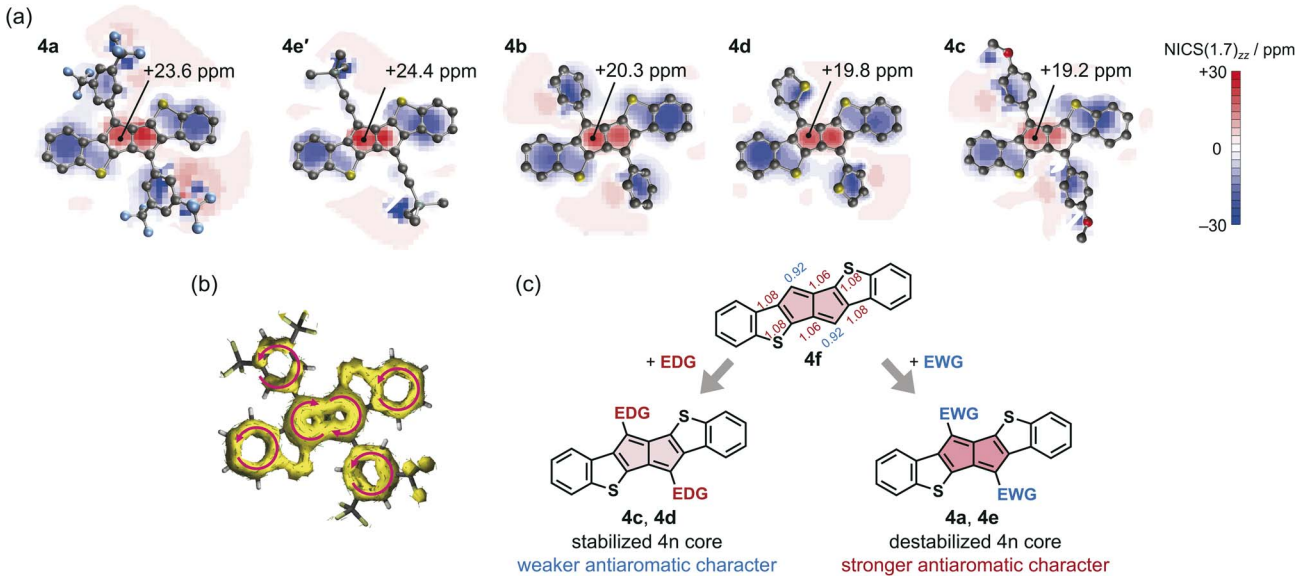

Fig. 5 Substituent-dependent antiaromatic character of benzothiophene-fused pentalenes **4a–e**. A model compound **4e′**, in which the TIPS groups were replaced with TMS groups, was used instead of **4e** to reduce computational costs. (a) NICS 2D plots at 1.7 Å of the *z* axis and NICS(1.7)$_{zz}$ values of **4a–d** and **4e′**. (b) ACID plot of **4a** (isosurface value = 0.03). NICS and ACID calculations were conducted at the M06-2X/6-31++G(2d,p) and M06-2X/6-31G(d), respectively, using the optimized geometries at the M06-2X/6-31++G(d) level of theory. The *xy* planes were set on the mean planes defined by the benzothiophene-fused pentalene frameworks. The magnetic field in the ACID calculations was chosen to be parallel to the *z* axis, which is oriented in a perpendicular direction to the paper plane and pointing towards the reader. Only the π-electron contribution was used. (c) Schematic representations based on the topological charge stabilization rule. For **4f**, NBO 2p$_z$ occupancies at each carbon atom are shown. The numbers with relatively high and low 2p$_z$ occupancies are shown in red and blue, respectively.

Single-crystal X-ray diffraction of **4e** unambiguously confirmed the formation of benzothiophene-fused pentalenes (Fig. 3c and S1–S2). The crystal structure of **4b** has been reported previously.[34] Both **4b** and **4e** featured a highly planar benzothiophene-fused pentalene core, forming slipped π–π stacking arrangements along the molecular long axis (Fig. S2). The peripheral C–C bonds of the pentalene cores displayed pronounced bond-length alternation, consistent with strong antiaromatic character. The C–C bonds fused to the thiophene rings were relatively short, indicating double-bond character.

The UV/vis/NIR absorption spectra of **4a–e** exhibited weak, broad first absorption bands at around 600–1100 nm, typical of cyclic 4n π-electron systems, along with a more intense second band around 500 nm (Fig. 4a). Compared with dibenzo[*a*,*e*]pentalene (**2**, R = SiMe$_3$, λ_{max} = 503 nm)[25] and dithieno[*a*,*e*]pentalene (**3**, R = SiMe$_3$, λ_{max} = 639 nm),[25] the first absorption bands of **4a–e** (λ_{max} at around 800 nm) were markedly red-shifted, reflecting enhanced antiaromatic character of the pentalene core and π-expansion. Cyclic voltammetry showed reversible oxidation and reduction waves (Fig. 4b), confirming their amphoteric redox behavior.

The redox potentials reflected the electronic nature of the substituents: the most electron-withdrawing **4a** exhibited $E_{1/2,ox}$ = +0.48 V and $E_{1/2,red}$ = −0.97 V (*vs.* Fc/Fc$^+$), whereas the electron-donating **4c** showed the half-wave potentials $E_{1/2,ox}$ = +0.16 V and $E_{1/2,red}$ = −1.36 V (*vs.* Fc/Fc$^+$), respectively. These results demonstrate that the electronic properties of benzothiophene-fused pentalene can be finely tuned by varying the substituents. The HOMO–LUMO gaps estimated from redox onsets (1.17–1.37 eV, Table S2) were significantly smaller than those of **2** (2.48 eV)[25] and **3** (1.87 eV),[25] consistent with the enhanced antiaromatic character and efficient π-conjugation.

To quantify the degree of antiaromatic character, the paratropicity strength, a magnetic descriptor of antiaromaticity, was estimated by computing the NICS(1.7)$_{zz}$ values[38] for **4a–d** and **4e′** at the M06-2X/6-31++G(2d,p)//M06-2X/6-31++G(d) level of theory (Fig. 5a).‡ All compounds exhibited large positive values in the range from +19.2 ppm to +24.4 ppm, confirming pronounced antiaromaticity relative to dibenzo[*a*,*e*]pentalene **2** (R = Ph, +3.8 ppm). The anisotropy of the induced current density (ACID) plot[39] for **4a** calculated at the same level of theory clearly indicated that a paramagnetic ring current exists along the 8-membered-ring periphery of the pentalene moiety (Fig. 5b). Notably, the trend in NICS(1.7)$_{zz}$ values, **4c** (+19.2 ppm) < **4d** (+19.8 ppm) < **4b** (+20.3 ppm) < **4a** (+23.6 ppm) < **4e′** (+24.4 ppm), intuitively correlates with the electron-withdrawing strength of the substituents. This result is consistent with recent observations in alkylthio-substituted dibenzo[*a*,*e*]pentalene and its sulfone analogue,[20e] and underscores the importance of the electronic effects of substituents in modulating antiaromaticity.

To rationalize these substituent effects, we applied the topological charge stabilization rule, originally proposed by Gimarc[40] and recently utilized by Wu *et al.*, to understand the positional effects of heteroatom doping on the paratropicity of indacene-based PAHs.[41] According to this rule, the 1,4-carbons of pristine pentalene possess partial positive character (δ^+); thus, electron-donating substituents stabilize the system, while electron-withdrawing groups destabilize it (Fig. 5c). Consequently, the former are expected to weaken, and the latter to enhance, the antiaromatic character. This interpretation is consistent with the

observed trend in NICS values and provides an intuitive explanation for the substituent-dependent modulation of the antiaromatic character of pentalene. These results demonstrate that the electronic effects of both the fused ring system and the substituents cooperatively determine the degree of antiaromatic character of the pentalene moiety. In particular, the introduction of strongly electron-withdrawing groups effectively enhances the antiaromatic character of the pentalene core.

Conclusions

In conclusion, we developed a versatile and general synthetic route to benzothiophene-fused pentalenes through a thiophene analogue of Brand's bicyclo[3.3.0]octadiene-2,6-dione intermediate. Pre-installation of the bicyclic five-membered-ring framework enabled efficient annulation of benzothiophene units and late-stage diversification at the 1,4-positions, overcoming the limitations of conventional approaches to hereroarene-fused pentalenes. The resulting compounds constitute a new family of stable yet strongly antiaromatic compounds, whose electronic and magnetic properties can be finely tuned by substituents. These findings provide a robust platform for understanding substituent effects on antiaromaticity and offer design principles for future functional materials based on antiaromatic π-systems.

This work was supported by JST CREST Grant Number JPMJCR23O2 (for A.F.), and JSPS KAKENHI Grant Numbers JP20H05864, JP21H01916, and JP24H00458 (for A.F.), and JP24KJ1436 (for R.I.). The authors thank the iCeMS Analysis Center for providing access to the NMR spectrometer. The synchrotron single-crystal X-ray diffraction measurements were performed at the BL02B1 beamline of SPring-8 with the approval of the Japan Synchrotron Radiation Research Institute (JASRI; project no. 2024A1699).

Author contributions

R. I.: investigation, methodology, formal analysis, data curation, funding acquisition, visualization, writing – original draft. K. Y.: conceptualization, supervision, writing – review & editing. A. F.: conceptualization, data curation, formal analysis, funding acquisition, project administration, supervision, visualization, writing – review & editing.

Conflicts of interest

There are no conflicts to declare.

Data availability

Data supporting this article are included in the supplementary information (SI). Supplementary information is available. See DOI: https://doi.org/10.1039/d5sc09325b.

CCDC 2504966 (**4e**) contains the supplementary crystallographic data for this paper.[42]

Notes and references

§ The yield of this intramolecular cyclization reaction was found to be sensitive to the type of ligand and base used in the reaction. The effect of the ligand and base is shown in Table S1.

¶ The proposed reaction mechanism for this ring-opening reaction is shown in Scheme S1.

‡ X-ray crystal data were available only for compounds **4b** and **4e**. Geometry optimizations were therefore performed for **4a–d** and **4e′**, and the optimized structures were used for further analyses. To reduce computational costs, a model compound **4e′**, in which the TIPS groups were replaced with TMS groups, was used instead of **4e**. Several density functionals were tested using **4e′** as a model system, given that NICS values are sensitive to even subtle differences in bond-length distributions, as noted in ref. 43. As a result, the M06-2X density functional gave the best agreement with the experimental C–C bond lengths of the pentalene core determined by X-ray crystallographic analysis. See the SI for details.

1 A. Minsky, A. Y. Meyer and M. Rabinovitz, *Tetrahedron*, 1985, **41**, 785–791.
2 I. Willner, J. Y. Becker and M. Rabinovitz, *J. Am. Chem. Soc.*, 1979, **101**, 395–401.
3 (*a*) W. T. Borden, E. R. Davidson and P. Hart, *J. Am. Chem. Soc.*, 1978, **100**, 388–392; (*b*) J. A. Jafri and M. D. Newton, *J. Am. Chem. Soc.*, 1978, **100**, 5012–5017; (*c*) M. Eckert-Maksić, M. Vazdar, M. Barbatti, H. Lischka and Z. B. Maksić, *J. Chem. Phys.*, 2006, **125**, 064310; (*d*) G. Hohlneicher, L. Packschies and J. Weber, *Phys. Chem. Chem. Phys.*, 2007, **9**, 2517–2530; (*e*) P. B. Karadakov, *J. Phys. Chem. A*, 2008, **112**, 7303–7309; (*f*) J. I.-C. Wu, Y. Mo, F. A. Evangelista and P. v. R. Schleyer, *Chem. Commun.*, 2012, **48**, 8437–8439.
4 (*a*) J. Wirz, A. Krebs, H. Schmalstieg and H. Angliker, *Angew Chem. Int. Ed. Engl.*, 1981, **20**, 192–193; (*b*) M. Ueda, K. Jorner, Y. M. Sung, T. Mori, Q. Xiao, D. Kim, H. Ottosson, T. Aida and Y. Itoh, *Nat. Commun.*, 2017, **8**, 346; (*c*) A. Kostenko, B. Tumanskii, Y. Kobayashi, M. Nakamoto, A. Sekiguchi and Y. Apeloig, *Angew. Chem., Int. Ed.*, 2017, **56**, 10183–10187.
5 Selected reviews:(*a*) A. Konishi and M. Yasuda, *Chem. Lett.*, 2021, **50**, 195; (*b*) C. Hong, J. Baltazar and J. D. Tovar, *Eur. J. Org Chem.*, 2022, e202101343.
6 (*a*) K. Hafner and H. U. Süss, *Angew Chem. Int. Ed. Engl.*, 1973, **12**, 575–577; (*b*) K. Hafner, R. Dönges, E. Goedecke and R. Kaiser, *Angew Chem. Int. Ed. Engl.*, 1973, **12**, 337–339; (*c*) R. Dönges, K. Hafner and H. J. Lindner, *Tetrahedron Lett.*, 1976, **17**, 1345–1348; (*d*) M. Suda and K. Hafner, *Tetrahedron Lett.*, 1977, **18**, 2449–2452; (*e*) T. Bally, S. Chai, M. Neuenschwander and Z. Zhu, *J. Am. Chem. Soc.*, 1997, **119**, 1869–1875.
7 H. Hopf, *Angew. Chem., Int. Ed.*, 2013, **52**, 12224–12226.
8 K. Brand, *Berichte Dtsch. Chem. Ges.*, 1912, **45**, 3071–3077.
9 (*a*) F. Xu, L. Peng, A. Orita and J. Otera, *Org. Lett.*, 2012, **14**, 3970–3973; (*b*) F. Xu, L. Peng, K. Shinohara, T. Morita, S. Yoshida, T. Hosoya, A. Orita and J. Otera, *J. Org. Chem.*, 2014, **79**, 11592–11608.
10 M. Saito, M. Nakamura, T. Tajima and M. Yoshioka, *Angew. Chem., Int. Ed.*, 2007, **46**, 1504–1507.
11 (*a*) Z. U. Levi and T. D. Tilley, *J. Am. Chem. Soc.*, 2009, **131**, 2796–2797; (*b*) Z. U. Levi and T. D. Tilley, *J. Am. Chem. Soc.*, 2010, **132**, 11012–11014; (*c*) J. Shen, D. Yuan, Y. Qiao,

X. Shen, Z. Zhang, Y. Zhong, Y. Yi and X. Zhu, *Org. Lett.*, 2014, **16**, 4924–4927.

12 (*a*) T. Kawase, A. Konishi, Y. Hirao, K. Matsumoto, H. Kurata and T. Kubo, *Chem.–Eur. J.*, 2009, **15**, 2653–2661; (*b*) A. Konishi, T. Fujiwara, N. Ogawa, Y. Hirao, K. Matsumoto, H. Kurata, T. Kubo, C. Kitamura and T. Kawase, *Chem. Lett.*, 2010, **39**, 300–301.

13 H. Zhang, T. Karasawa, H. Yamada, A. Wakamiya and S. Yamaguchi, *Org. Lett.*, 2009, **11**, 3076–3079.

14 (*a*) A. S. K. Hashmi, M. Wieteck, I. Braun, P. Nösel, L. Jongbloed, M. Rudolph and F. Rominger, *Adv. Synth. Catal.*, 2012, **354**, 555–562; (*b*) M. M. Hansmann, M. Rudolph, F. Rominger and A. S. K. Hashmi, *Angew. Chem., Int. Ed.*, 2013, **52**, 2593–2598; (*c*) T. Wurm, E. C. Rüdiger, J. Schulmeister, S. Koser, M. Rudolph, F. Rominger, U. H. F. Bunz and A. S. K. Hashmi, *Chem.–Eur. J.*, 2018, **24**, 2735–2740; (*d*) S. Tavakkolifard, K. Sekine, L. Reichert, M. Ebrahimi, K. Museridz, E. Michel, F. Rominger, R. Babaahmadi, A. Ariafard, B. F. Yates, M. Rudolph and A. S. K. Hashmi, *Chem.–Eur. J.*, 2019, **25**, 12180–12186.

15 P. R. Fuentes, M. v. W. Rekowski, W. B. Schweizer, J. P. Gisselbrecht, C. Boudon and F. Diedrich, *Org. Lett.*, 2012, **14**, 4066–4069.

16 C. Chen, M. Harhausen, R. Liedtke, K. Bussmann, A. Fukazawa, S. Yamaguchi, J. L. Petersen, C. G. Daniliuc, R. Fröhlich, G. Kehr and G. Erker, *Angew. Chem., Int. Ed.*, 2013, **52**, 5992–5996.

17 T. Maekawa, Y. Segawa and K. Itami, *Chem. Sci.*, 2013, **4**, 2369–2373.

18 K. Takahashi, S. Ito, R. Shintani and K. Nozaki, *Chem. Sci.*, 2017, **8**, 101–107.

19 Y. Wu, Y. Wang, J. Chen, G. Zhang, J. Yao, D. Zhang and H. Fu, *Angew. Chem., Int. Ed.*, 2017, **56**, 9400–9404.

20 (*a*) J. Wilbuer, D. C. Grenz, G. Schnakenburg and B. Esser, *Org. Chem. Front.*, 2017, **4**, 658–663; (*b*) D. C. Grenz, M. Schmidt, D. Kratzert and B. Esser, *J. Org. Chem.*, 2018, **83**, 656–663; (*c*) M. Hermann, T. Böttcher, M. Schorpp, S. Richert, D. Wassy, I. Krossing and B. Esser, *Chem.–Eur. J.*, 2021, **27**, 4964–4970; (*d*) M. Schmidt, L. A. Vicente, M. T. González, L. A. Zotti, B. Esser and E. Leary, *Chem.–Eur. J.*, 2024, **30**, e202400935; (*e*) M. Hermann, S. M. A. Battisti and B. Esser, *Asian J. Org. Chem.*, 2025, **14**, e202500231.

21 (*a*) M. Hermann, D. Wassy, D. Kratzert and B. Esser, *Chem.–Eur. J.*, 2018, **24**, 7374–7387; (*b*) D. Wassy, M. Pfeifer and B. Esser, *J. Org. Chem.*, 2020, **85**, 34–43; (*c*) D. Wassy, M. Hermann, J. S. Wössner, L. Frédéric, G. Pieters and B. Esser, *Chem. Sci.*, 2021, **12**, 10150–10158; (*d*) J. S. Wössner, D. Wassy, A. Weber, M. Bovenkerk, M. Hermann, M. Schmidt and B. Esser, *J. Am. Chem. Soc.*, 2021, **143**, 12244–12252; (*e*) J. S. Wössner, J. Kohn, D. Wassy, M. Hermann, S. Grimme and B. Esser, *Org. Lett.*, 2022, **24**, 983–988; (*f*) M. Hermann, D. Wassy, J. Kohn, P. Seitz, M. U. Betschart, S. Grimme and B. Esser, *Angew. Chem., Int. Ed.*, 2021, **60**, 10680–10689; (*g*) P. Seitz, L. Rzesny, D. Busse, X. Xiang, M. Hermann, L. Estaque, G. Pieters and B. Esser, *J. Am. Chem. Soc.*, 2025, **147**, 41610–41619; (*h*) A. Gupta, P. Seitz, M. Hermann, B. Esser and R. Naaman, *Adv. Funct. Mater.*, 2025, DOI: 10.1002/adfm.202523339.

22 (*a*) T. Kawase, T. Fujiwara, C. Kitamura, A. Konishi, Y. Hirao, K. Matsumoto, H. Kurata, T. Kubo, S. Shinamura, H. Mori, E. Miyazaki and K. Takimiya, *Angew. Chem., Int. Ed.*, 2010, **49**, 7728–7732; (*b*) M. Nakano, I. Osaka, K. Takimiya and T. Koganezawa, *J. Mater. Chem. C*, 2013, **2**, 64–70; (*c*) M. Nakano, I. Osaka and K. Takimiya, *J. Mater. Chem. C*, 2015, **3**, 283–290; (*d*) G. Dai, J. Chang, W. Zhang, S. Bai, K.-W. Huang, J. Xu and C. Chi, *Chem. Commun.*, 2014, **51**, 503–506; (*e*) G. Dai, J. Chang, X. Shi, W. Zhang, B. Zheng, K.-W. Huang and C. Chi, *Chem.–Eur. J.*, 2014, **21**, 2019–2028; (*f*) G. Dai, J. Chang, J. Luo, S. Dong, N. Aratani, B. Zheng, K. Huang, H. Yamada and C. Chi, *Angew. Chem., Int. Ed.*, 2016, **55**, 2693–2696; (*g*) G. Dai, J. Chang, L. Jing and C. Chi, *J. Mater. Chem. C*, 2016, **4**, 8758–8764; (*h*) M. Hermann, R. Wu, D. C. Grenz, D. Kratzert, H. Li and B. Esser, *J. Mater. Chem. C*, 2018, **6**, 5420–5426.

23 (*a*) J. Sprachmann, T. Wachsmuth, M. Bhosale, D. Burmeister, G. J. Smales, M. Schmidt, Z. Kochovski, N. Grabicki, R. Wessling, E. J. W. List-Kratochvil, B. Esser and O. Dumele, *J. Am. Chem. Soc.*, 2023, **145**, 2840–2851; (*b*) P. Seitz, M. Bhosale, L. Rzesny, A. Uhlmann, J. S. Wössner, R. Wessling and B. Esser, *Angew. Chem., Int. Ed.*, 2023, **62**, e202306184.

24 C. K. Frederickson, L. N. Zakharov and M. M. Haley, *J. Am. Chem. Soc.*, 2016, **138**, 16827–16838.

25 J. Usuba, M. Hayakawa, S. Yamaguchi and A. Fukazawa, *Chem.–Eur. J.*, 2021, **27**, 1638–1647.

26 C. Hu and Q. Zhang, *Chin. J. Chem.*, 2013, **31**, 1404–1408.

27 S. Kato, S. Kuwako, N. Takahashi, T. Kijima and Y. Nakamura, *J. Org. Chem.*, 2016, **81**, 7700–7710.

28 H. Oshima, A. Fukazawa and S. Yamaguchi, *Angew. Chem., Int. Ed.*, 2017, **56**, 3270–3274.

29 (*a*) B. Yuan, J. Zhuang, K. M. Kirmess, C. N. Bridgmohan, A. C. Whalley, L. Wang and K. N. Plunkett, *J. Org. Chem.*, 2016, **81**, 8312–8318; (*b*) A. Konishi, S. Satake and M. Yasuda, *Chem. Lett.*, 2020, **49**, 589–592.

30 X. Yin, Y. Li, Y. Zhu, Y. Kan, Y. Li and D. Zhu, *Org. Lett.*, 2011, **13**, 1520–1523.

31 T. Gazdag, P. J. Mayer, P. P. Kalapos, T. Holczbauer, O. E. Bakouri and G. London, *ACS Omega*, 2022, **7**, 8336–8349.

32 (*a*) A. Konishi, Y. Okada, M. Nakano, K. Sugisaki, K. Sato, T. Takui and M. Yasuda, *J. Am. Chem. Soc.*, 2017, **139**, 15284–15287; (*b*) A. Konishi, Y. Okada, R. Kishi, M. Nakano and M. Yasuda, *J. Am. Chem. Soc.*, 2019, **141**, 560–571; (*c*) A. Konishi, K. Horii, H. Iwasa, Y. Okada, R. Kishi, M. Nakano and M. Yasuda, *Chem.–Asian J.*, 2021, **16**, 1553–1561; (*d*) K. Horii, A. Nogata, Y. Mizuno, H. Iwasa, M. Suzuki, K. Nakayama, A. Konishi and M. Yasuda, *Chem. Lett.*, 2022, **51**, 325–329; (*e*) Y. Mizuno, A. Nogata, M. Suzuki, K. Nakayama, I. Hisaki, R. Kishi, A. Konishi and M. Yasuda, *J. Am. Chem. Soc.*, 2023, **145**, 20595–20609.

33 Q. Jiang, T. Wang, Y. Han, H. Wei, Y. Deng, Y. Geng and C. Chi, *Angew. Chem., Int. Ed.*, 2025, e202513158.
34 R. Kuwata, T. Imanishi, S. Hasegawa, Z. Wang, J. Usuba, K. Yasui, M. U. G. Khan, J. I. Wu, Y. Uetake and A. Fukazawa, *ChemRxiv*, 2025, DOI: 10.2634/chemrxiv-2025-l8c87-v2.
35 R. M. Moriarty, M. P. Duncan, R. K. Vaid and O. M. Prakash, *Org. Synth.*, 1990, **68**, 175.
36 T. Mukaiyama and K. Saigo, *Chem. Lett.*, 1973, **2**, 479–482.
37 H. Zaimoku, T. Hatta, T. Taniguchi and H. Ishibashi, *Org. Lett.*, 2012, **14**, 6088–6091.
38 Z. Chen, C. S. Wannere, C. Corminboeuf, R. Puchta and P. v. R. Schleyer, *Chem. Rev.*, 2005, **105**, 3842–3888.
39 D. Geuenich, K. Hess, F. Köhler and R. Herges, *Chem. Rev.*, 2005, **105**, 3758–3772.
40 B. M. Gimarc, *J. Am. Chem. Soc.*, 1983, **105**, 1979–1984.
41 S. Jalife and J. I. Wu, *J. Org. Chem.*, 2025, **90**, 4012–4017.
42 CCDC 2504966: Experimental Crystal Structure Determination, 2026, DOI: 10.5517/ccdc.csd.cc2q2mct.
43 L. J. Karas, S. Jalife, R. V. Viesser, J. V. Soares, M. M. Haley and J. I. Wu, *Angew. Chem., Int. Ed.*, 2023, **62**, e202307379.